Virtualization of Elastic Optical Networks and Regenerators with Traffic Grooming

K. D. R. Assis*[1], A. F. Santos[2], R. C. Almeida Jr[3], M. J. Reed[4], B. Jaumard[5], and D. Simeonidou[6]

[1] Federal University of Bahia, Electrical and Computer Engineering Department, Rua Prof. Aristides Novis nº 02 Federação, Salvador, Bahia, Brazil
[2] Science and Technology Center on Energy and Sustainability, Federal University of Recôncavo da Bahia, Feira de Santana, Bahia, Brazil
[3] Department of Electronics and Systems, Federal University of Pernambuco, Recife, Pernambuco, Brazil
[4] School of Computer Science and Electronic Eng., University of Essex, UK
[5] Department of Computer Science and Software Engineering, Concordia University, Montreal, QC H4B 1R6, Canada
[6] Smart Internet Lab and High Performance Networks group (HPN), University of Bristol, Bristol, UK
* Corresponding author: karcius.assis@ufba.br

Compiled November 18, 2020

An elastic optical network (EON) plays an important role in transport technology for virtualization of networks. A key aspect of EONs is to establish lightpaths (virtual links) with exactly the amount of spectrum that is needed and with the possibility of grooming, the process of grouping many small traffic flows into larger units, creating a super-lightpath. Grooming eliminates the need for many guard bands between lightpaths and also saves transceivers; however, it often leads to the need to perform O/E/O conversions to multiple-data-rate optical signals at intermediate nodes. The aim of this paper is to provide a mixed-integer linear programming (MILP) formulation, as well as heuristic and meta-heuristic approaches, for the design of multiple virtual optical networks (VONs) in an elastic optical substrate network with bandwidth-variable lightpaths, modulation format constraints and virtual elastic regenerator placement. Traffic grooming is allowed inside each VON and a distance-adaptive modulation-format technique is employed to guarantee efficiency in terms of bandwidth for a physical substrate, subject to several virtual topologies. A reduced (EQ2) MILP formulation without grooming capability is also proposed for comparison. The complete MILP formulation jointly solves the virtual topology design, the regenerator placement, grooming as well as the routing, modulation and spectrum assignment (RMSA) problems. The reduced (EQ2) MILP formulation, heuristics and meta-heuristic, on the other hand, separate the virtual topology design problem from the RMSA problem. It is shown that the grooming approach can provide good results, since it solves the problem for a complete design when compared to the approach without grooming. Furthermore, heuristic solutions for large networks are proposed, which present good performance (in terms of saving spectrum) for the design with large instances.

http://dx.doi.org/10.1364/ao.XX.XXXXXX

1. INTRODUCTION

The problem of virtual topology design (VTD), or logical topology design (LTD), for optical networks has been studied for some time [1]. The rationale for using a virtual topology on top of an optical infrastructure has been investigated previously. For example, the number of transceivers in an optical network cannot be increased indefinitely without running into a connectivity bottleneck. The origin of the bottleneck are the resource limitations within the network (fibers, optical spectrum, regenerators and optical transceivers) [2]. This problem has become more complex with the possibility of having several virtual topologies for the same physical substrate, when network virtualization is used, in which multiple independent virtual topologies share resources [3–5]. Also with the 5th generation of mobile networking (5G) on our doorstep, optical network operators are reorganizing their network infrastructures so that they can deploy different topologies on the same physical infrastructure on demand, where network function virtualization (NFV) can be enabled by segmenting the physical resources based on the requirements of the application level [6]. Furthermore, the recent developments in the field of elastic optical networks (EON) have led to renewed interest in the study of virtualization and

a number of researchers have reported the use of virtualization with EONs as a solution to meet customer needs [3–5].

Turning now to the routing strategies, traffic grooming allows the aggregation of traffic at intermediate nodes from different source-destination node pairs over a virtual layer. Such grooming techniques allow the establishment of optical paths carrying several connections in a contiguous block of spectrum without inserting guard bands in between, therefore minimizing the spectrum usage or the number of transmitters.

Despite the proven benefits of grooming, previous studies have not treated in much detail the combination of routing with grooming in a (EQ3) virtual topology.

In particular it is not clear what factors in virtual topologies affect the design when grooming is included. In addition, there still remain important challenges regarding hardware level virtualization in optical networks and [7] provides evidence to support our claim for a detailed study (R3Q1) in that area. For example, rate and modulation-format adaptive transponders will enable spectrum-efficient networking; however, there might be stranded hardware resources when they are used at lower rates. There is a lack of study about the capability for the sharing in the design of an adaptive transponder, which is a fundamental concept of virtualization. This demonstrates the need to understand virtualization within the design of EONs (R3Q2), including the use of Optical-Electrical-Optical (OEO) regeneration functionality. The above supports the need to study virtualisation with routing and grooming to design EONs in a scalable and cost effective manner [7].

This paper presents a study through mixed-integer linear programming (MILP) and heuristics of how to map virtual topologies on an optical elastic substrate network, subject to certain constraints to such topologies, notably the flow conservation and spectrum continuity and contiguity on the routing and spectrum assignment (RSA) problem [8]. Modulation format constraints and substrate resources (nodes and links) constraints are also considered [9, 10].

In this study multi-flow optical transponders and elastic regenerators [7, 11] are used to support optical network virtualization and improve energy and spectrum efficiency through the employment of different line rates in elastic lightpaths [12].

This paper differs from other works in the literature [3–5], as a mapping of virtual optical networks (VONs) over a physical substrate or virtualization is proposed considering grooming of traffic for each virtual topology. Therefore, the MILP formulation searches for the most appropriate lightpaths (referred to as virtual links in this work), based on the traffic matrix of each virtual topology.

This paper examines the emerging role of virtualization in the context of some important aspects, specifically: 1) a comparison between the grooming and non-grooming approaches, showing the advantages of grooming; 2) the role of virtual elastic regenerators (VERs), [7], in virtualization design as a solution for efficiently regenerating various bandwidth superchannels (because they are cost-efficient in relation to traditional dedicated data-rate regenerators or rate-adaptive regenerator [13]); 3) proposing heuristics to guide the solution for large instances as this type of problem is non-deterministic polynomial time (NP) complete [14]; 4) demonstrating MILPs as benchmarks for the design problem of VONs with other objectives considering elastic regenerators in constraints, for example, a survivability study, such as that presented in [12, 15, 16].

The remaining of this paper is organized as follows. Some statements and related works are presented in Section 2 with the MILP formulation presented in Section 3. The related heuristic algorithms are proposed in Section 4 and simulation results are analyzed in Section 5. Finally, the paper is concluded in Section 6.

2. VONS, GROOMING, REGENERATORS AND RELATED WORKS

Virtualization is defined as the composition of multiple isolated VONs simultaneously coexisting over the same physical substrate. The EON is an attractive transport technology for virtualization due to the possibility of achieving efficient mapping of virtual resources onto the shared physical substrate. Fig. 1 illustrates the mapping of two VONs over a same physical substrate.

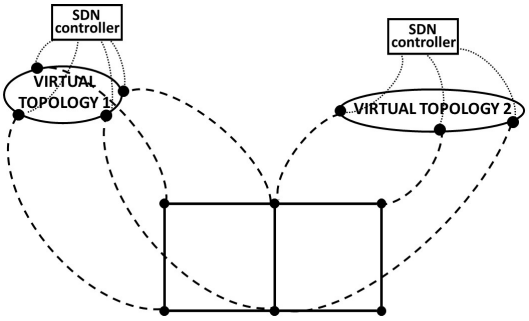

Fig. 1. The mapping of two VONs over a same physical substrate.

Optical network virtualization can support the end-to-end service provisioning through software defined network (SDN)-enabled virtualization. This virtualization will enable the rapid deployment of multi-tenant, application-specific and customized virtual infrastructures (VIs). In the optical network, each VON can have its own control plane to enable the provisioning of dynamic, adaptive and fault-tolerant optical network services [15].

For example, in Fig. 1 a SDN controller manages each VON and each one can have different applications, services etc [17]. However, researchers have not dealt with the grooming of multiple virtual topologies, therefore, they have not treated the complete design. For VON applications, the ability to save spectrum, transceivers and regenerators (resources) is very important, especially when they are limited resources.

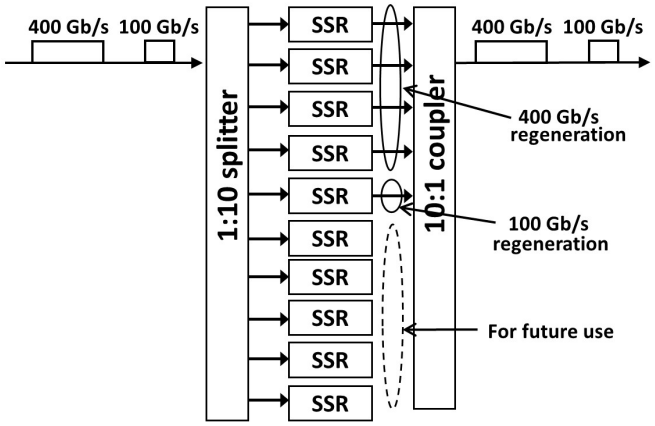

Fig. 2. VER architecture,[11]

A. Grooming

In an EON substrate, it may not be feasible to set up virtual links between all nodes pairs due to a limited number of resources such as optical transmitters, receivers and regenerators. Therefore, the design of EONs with grooming poses several challenges. Inspired by the functionality of traffic grooming in wavelength-division multiplexing (WDM), in this paper a traffic grooming scheme is applied in EONs with multiple VONs. The multiple wavelength channels in one fiber, which are defined in traditional WDM networks, no longer exist; instead, bandwidth-variable wavebands share the entire spectrum in one fiber in a "Gridless" manner. In fact, EON proposes various grids that are different from the 50-GHz fixed grid (EQ18) of traditional WDM systems. The minimum defined by the ITU-T G.709 is 12.5 GHz flexible grid. Therefore, the virtual links in traffic-grooming of EONs are also bandwidth-variable. In this scheme, multiple low-speed traffic requests in virtual connections at the electrical layer are groomed into bandwidth-variable virtual links, and then the virtual links are mapped to the routing in the physical substrate or optical layer. Beside that, when grooming is used, a considerable fraction of bandwidth can be saved without the constraint of fixed "grids", especially for sub-wavelength services where the transponder's high capacity is not fully used [18].

Each pair of adjacent sub-wavelength paths need guard bands between them (EQ4). This may result in significant spectrum overhead [19]. Therefore, it is interesting to groom multiple small traffic services into a BV-transponder and switch them together as a whole [18, 20, 21].

B. Virtual Regenerators

The use of *virtual regenerators* allows a new cost-efficient architecture as shown with a simple example in Fig. 2 which consists of an array of spectrum-selective subchannel regenerators (SSRs) [11]. This architecture provides scalability with respect to distance (EQ5) by regenerating multiple data-rate optical signals in a cost-effective manner [11]. The key to this solution is the VER. It can regenerate a range of different bandwidth optical superchannels. Such a VER can regenerate inverse multiplexed discrete and Nyquist WDM superchannels by selectivly choosing the appropriate SSRs and aggregating as necessary. For example, in Fig. 2, four tightly aligned Nyquist WDM subchannels, forming a 400 Gb/s superchannel, are regenerated by four 100 Gb/s SSRs; whereas a single SSR can also be selected for a single 100 Gb/s using the same architecture.

C. Related Works and Methodology

In 1996, Ramaswami *et al* [1] described a study where a logical or virtual topology is designed over a WDM network. The problem is divided into the design of the virtual topology and the solution of the routing and wavelength assignment problem (EQ13). There is a MILP, but it considers only the virtual design in the first phase (EQ14). WDM technology is used in the second phase (EQ15). In the mapping strategy, (EQ6, EQ16, R3Q3) the virtual topology has exactly the same number of nodes as the physical topology (EQ17), similar to the strategy used in this paper. Currently, numerous studies have attempted the virtualization with EONs. The authors in [3–5] propose mapping strategies using MILP formulation and/or heuristics with pre-defined routes and with/without modulation format constraints. However, no grooming is implemented in the formulations/heuristics. Recently, [5] and [22] have also proposed MILP formulations for the virtualization problem over elastic optical networks, but also they do not study the grooming approach. Previous studies, as that presented in [11], have reported a demonstration of virtualization with VERs and [12] is a clear illustration of the importance of the topic; it draws on survivability and energy efficiency study with MILP and heuristics for virtualization in EONs. In [13], the authors investigate the combined traffic grooming and regenerator placement problem with the goal of minimizing cost for the first time. They provide a detailed ROADM node architecture, formulating the combined traffic grooming and regenerator placement problem. However, (R3Q3) the architecture they consider is for WDM networks with non elastic regenerators. In [23] the authors report a heuristic for calculating the minimal VER placement ploblem, routing, and the least congestion resources assignment in a translucent EON based on Nyquist WDM superchannels; however, there is not a exact formulation to solve the problem.

The MILP proposed in this paper seeks to address the virtualization of EONs with grooming and taking into account the elastic regenerators. The MILP also addresses jointly EQ7 the routing, modulation level, and spectrum assignment (RMSA) problem in physical substrates for several virtual topologies. This paper provides a significant contribution by using grooming in each VON to route the demands by flow balance equations in the VONs and the physical substrate. Since the grooming is applied for each virtual topology, there is no sharing of traffic between the T tenant VONs, but only the physical substrate, consequently each tenant may be able to easily reconfigure its own VON.

Fig. 3 shows the proposed design methodology. The VONs are activated requiring grooming and RMSA that aims to minimize the maximum spectrum slot index (C). Table 1 shows a summary of contributions towards EONs with virtualization available in the literature and the contributions of the proposals in this paper.

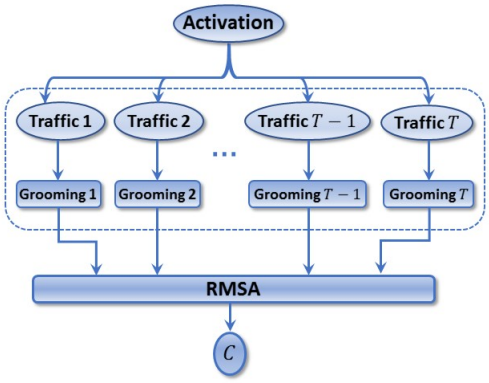

Fig. 3. Methodology of Design

3. MILP FORMULATION

A few MILP formulations have been proposed to solve the virtualization problem over EONs, but to the best of the authors' knowledge, none have tackled the complete case (virtualization, grooming, virtualized regenerator placement and assignment, as well as routing spectrum and modulation assignment). The authors introduce a MILP formulation capable of providing the optimal solution, in terms of spectrum, for the VONs that require allocation, also subject to reducing the need for virtual

Table 1. Summary of the contributions of the papers available in the literature and the main contribution of our proposals in this paper.

Reference	Virtualization	Multiple VONs	Grooming	EON	Regen. Placement	MILP /ILP	Heuristic	Survivability / Energy Efficiency
[1]	X	-	X	-	-	X	X	-
[3–5, 22]	X	X	-	X	-	X	X	-
[11]	X	-	-	X	X	-	-	-
[12]	X	X	-	X	X	X	X	X
[13]	X	-	X	-	X	X	X	-
[23]	X	-	X	X	X	-	X	-
Our Proposals	X	X	X	X	X	X	X	-

regenerators (EQ19).

A. Scientific Notation

- s and d denote the source and destination nodes of the traffic demands D in the network, respectively.
- i and j denote originating and terminating nodes of a heterogeneous bandwidth lightpath, respectively.
- m and n denote endpoints of a physical link in the network.
- z denotes the kind of modulation format from a set of M available modulation formats, $z \in \{1, 2..M\}$.
- t denotes the VON from a set of T virtual topologies, $t \in \{1, 2..T\}$.

B. Given Parameters

- $G = (N, E)$: graph representing the topology of the physical network with N being the set of nodes and E the set of links.
- $\Lambda^{sd,t}$: a traffic matrix element, with the traffic injected into node s and destined for node d in the virtual topology t.
- F: the minimum spectrum width between wavebands (guard band).
- Ω: slot width.
- d_{mn}: distance between the nodes m and n on physical topology.
- η_z: spectral efficiency of the modulation format z in which $z \in 1, \ldots, M$.
- d_z: maximum reach for a lightpath using modulation format z in which $z \in 1, \ldots, M$.
- R: regeneration capacity for a SSR. In this paper R=100 Gb/s.
- χ: An arbitrarily large number (greater than the number of slots available) which allows formation of constraints from integer slot allocation variables.

C. Definition of Variables

- $v^{ij,t}$: lightpath bandwidth (in Gb/s) from node i to node j in the virtual topology t.
- $\lambda_{ij}^{sd,t}$: traffic flow (in Gb/s) from source s to destination d carried on lightpath from node i to node j in the virtual topology t.
- $b_{ij,t}$: binary variable to indicate if a virtual link exists between a node pair on virtual topology t. It is 1 if there is a virtual link from node i to node j on t. Otherwise it is 0. In this paper, it is assumed that there can be at most one virtual link between a pair of nodes on t.
- $nl^{ij,t}$: number of SSR blocks with a certain bit rate capacity (R Gb/s) used by an elastic lightpath from i to j in the virtual topology t.
- ri_k: number of splitters requested in input of node k from all T VONs and their elastic lightpaths with regeneration in the node k.
- ro_k: number of couplers requested in output of node k from all T VONs and their elastic lightpaths with regeneration in the node k.
- $SSR_k = max(ri_k, ro_k)$: number of SSRs needed in node k.
- rt_k: total number of splitters/couplers requested in node k.
- $p^{ij,t}$: number of slots of an elastic lightpath from i to j in the physical substrate for virtual topology t.
- $P_{mn}^{ij,t}$: amount of bandwidth (in slots) that a lightpath from node i to node j in virtual topology t uses in a fiber link mn.
- $A_{mn}^{ij,t}$: routing indicator. A binary variable to indicate whether the lightpath from node i to node j in the virtual topology t passes through a link m-n. $A_{mn}^{ij,t}$ equals to 1 if $P_{mn}^{ij,t} > 0$; equals to 0 if $P_{mn}^{ij,t} = 0$.
- $\epsilon_z^{ij,t}$: modulation format indicator. A binary variable that indicates if an elastic lightpath from node i to node j in the virtual topology t employs the modulation format z.
- $s^{ij,t}$: starting frequency slot for lightpath i-j in t.
- $W_{ij}^{ku,t}$ a binary variable. It is 1 if the starting frequency of lightpath i-j is smaller than the starting frequency of lightpath k-u. (i.e, $s^{ij,t} < s^{ku,t}$) and 0 otherwise.

- C: largest used frequency slot index.

D. MILP formulation with Traffic Grooming

In this subsection the complete MILP formulation is presented. The objective is to minimize the maximum utilized spectrum slot index, C. However, we are also interested in minimizing the number of SSRs to set up the VONs. In the future, we might need to set up a new elastic lightpath, which is unknown beforehand, so saving SSRs increase the possibilities to set up a lightpath for future use. This issue is then solved with the objective function in Eq. (1), where θ is chosen small enough so that the added term does not influence the aim of maximizing the residual slot capacity for future demands. Then, the objective function below minimizes the maximum utilized spectrum slot index and at the same time minimizes the total number of SSRs used for the required virtual topologies.

$$\min \quad (C + \theta . \sum_{k} SSR_k) \tag{1}$$

– ***subject to:***

Grooming constraints:

$$\sum_{j} \lambda_{ij}^{sd,t} - \sum_{j} \lambda_{ji}^{sd,t} = \begin{cases} \Lambda^{sd,t} & if \quad i = s \\ -\Lambda^{sd,t} & if \quad i = d \\ 0 & if \quad i \neq d \end{cases} \quad \forall (s,d), i, t \tag{2}$$

$$\lambda_{ij}^{sd,t} \leq b_{ij,t} . \Lambda^{sd,t} \quad \forall (s,d), t \tag{3}$$

$$\sum_{sd} \lambda_{ij}^{sd,t} = v^{ij,t} \quad \forall (i,j), t \tag{4}$$

Regeneration constraints:

$$\lceil \frac{v^{ij,t}}{R} \rceil \leq nl^{ij,t} \quad \forall (i,j), t \tag{5}$$

$$\sum_{i,t} nl^{ik,t} = ri_k \quad \forall k \tag{6}$$

$$\sum_{j,t} nl^{kj,t} = ro_k \quad \forall k \tag{7}$$

$$max(ri_k, ro_k) = SSR_k \quad \forall k \tag{8}$$

Virtual link bandwidth setting and modulation format assignment:

$$p^{ij,t} \geq \frac{v^{ij,t}}{\Omega . \eta_z} - \left(1 - \epsilon_z^{ij,t}\right) . \chi \qquad \forall (i,j), t, z \tag{9}$$

$$p^{ij,t} \leq \frac{v^{ij,t}}{\Omega . \eta_z} + 1 + \left(1 - \epsilon_z^{ij,t}\right) . \chi \qquad \forall (i,j), t, z \tag{10}$$

$$\sum_{z} \epsilon_z^{ij,t} \leq 1 \qquad \forall (i,j), t \tag{11}$$

$$p^{ij,t} \leq \chi . \sum_{z} \epsilon_z^{ij,t} \qquad \forall (i,j), t \tag{12}$$

$$\frac{v^{ij,t}}{\chi} \leq \sum_{z} \epsilon_z^{ij,t} \leq \chi . v^{ij,t} \qquad \forall (i,j), t \tag{13}$$

Slot flow conservation, link usage indicator and modulation format distance requirement:

$$\sum_{n} P_{mn}^{ij,t} - \sum_{n} P_{nm}^{ij,t} = \begin{cases} p^{ij,t} & m = i \\ -p^{ij,t} & m = j \\ 0 & m \neq i,j \end{cases} \quad \forall (i,j), m, t \tag{14}$$

$$C \geq s^{ij,t} + p^{ij,t} \qquad \forall (i,j), t \tag{15}$$

$$A_{mn}^{ij,t} \geq P_{mn}^{ij,t} / \chi \qquad \forall (i,j), (m,n), t \tag{16}$$

$$A_{mn}^{ij,t} + A_{m\ell}^{ij,t} \leq 1 \qquad \forall (i,j), (m,n) \neq (m,\ell), t \tag{17}$$

$$\sum_{mn} A_{mn}^{ij,t} . d_{mn} \leq \sum_{z} d_z . \epsilon_z^{ij,t} \qquad \forall (i,j), t \tag{18}$$

Spectrum continuity and contiguity requirements:

$$A_{mn}^{ij,t_p} + A_{mn}^{ku,t_q} - 1 \leq W_{ku,t_q}^{ij,t_p} + W_{ij,t_p}^{ku,t_q} \leq 1$$
$$(i,j), t_p \in T, (k,u), t_q \in T, (i,j,t_p) \neq (k,u,t_q) \quad \forall i,j,k,u \tag{19}$$

EQ8

$$s^{ij,t_p} + p^{ij,t_p} + F \leq s^{ku,t_q} + \chi \cdot \left(1 - W_{ku,t_q}^{ij,t_p}\right)$$
$$(i,j), t_p \in T, (k,u), t_q \in T, (i,j,t_p) \neq (k,u,t_q) \quad \forall i,j,k,u \tag{20}$$

$$s^{ku,t_q} + p^{ku,t_q} + F \leq s^{ij,t_p} + \chi \cdot \left[1 - W_{ij,t_p}^{ku,t_q}\right]$$
$$(i,j), t_p \in T, (k,u), t_q \in T, (i,j,t_p) \neq (k,u,t_q) \quad \forall i,j,k,u \tag{21}$$

Unfortunately, Eq. (8) is non-linear. However, it may be replaced by constraints (22)-(25) that follow, where τ is a binary variable, and thus convert the MILP formulation into a linear problem.

$$SSR_k \geq ri_k \qquad \forall k \tag{22}$$

$$SSR_k \geq ro_k \qquad \forall k \tag{23}$$

$$SSR_k \leq ri_k + \chi . \tau \qquad \forall k \tag{24}$$

$$SSR_k \leq ro_k + \chi . (1 - \tau) \quad \forall k \tag{25}$$

Eq. (2) expresses traffic flow conservation at the nodes of a virtual link in t. The component of traffic offered onto a virtual link due to a node pair can be at most the amount of traffic flows between the node pair. This fact is captured by constraint (3). The sum of the traffic due to all (s,d) node pairs in t that is routed through virtual link $i-j$ is described in Eq. (4).

From (5) until (8) determine the number of SSRs. In (5), $nl^{ij,t}$ is assigned with the integer number indicating the number of SSRs required by the virtual link $i-j$ on t. For all t VONs, Eq. (6) indicates the total number of splitters in entering node and Eq. (7) indicates the total number of couplers in exiting node. Therefore, Eq. (8) indicates the total number of SSRs requested in each node of the substrate elastic optical network.

Constraints from (9) to (13) assure that a single modulation format is assigned to any virtual link in the network. The conservation of slots at nodes of the substrate network is expressed by Eq. (14), which asserts that the slots are added at the source node of the virtual link, dropped at the destination node or entirely bypassed at intermediate nodes. Notice that the slots of a virtual link that passes through a node in the substrate network have to be entirely switched to a single output link. Constraint (15), along with the Objective Function, is used to minimize the maximum number of spectrum slots used among all demands.

Constraint (16) is responsible for setting the value of $A_{mn}^{ij,t}$, which is set to one whenever traffic from the virtual link $i-j$ in t is routed through the physical link mn. Constraint (17) guarantees that a virtual link is routed along at most one of the node output fibers (i.e. optical multicasting is not allowed). Constraint (18) prevents any established lightpath from exceeding the distance limits imposed by its assigned modulation format.

For the continuity and contiguity requirements in the spectrum assignment, let the binary variable W_{ku,t_q}^{ij,t_p} be defined so that it is equal to 1 if the starting frequency slot of virtual link $i-j$ in t_p is smaller than the starting frequency slot of virtual link $k-u$ in t_q (i.e, $s^{ij,t} < s^{ku,t}$) and 0 otherwise. Constraint (19) guarantees that, if a virtual link $i-j$ in t_p and $k-u$ in t_q share any fiber in the network, ex. m-n, then $A_{mn}^{ij,t_p} = A_{mn}^{ku,t_q} = 1$ and, therefore, $W_{ku,t_q}^{ij,t_p} + W_{ij,t_p}^{ku,t_q} = 1$, which states that either W_{ku,t_q}^{ij,t_p} or W_{ij,t_p}^{ku,t_q} is equal to one and the other is equal to zero. Therefore, together with constraints (20) and (21), one can guarantee that their spectra do not overlap, in which F is the assumed filter guard band. On the other hand, if the virtual link $i-j$ in t_p and $k-u$ in t_q do not share any fiber in the network, then A_{mn}^{ij,t_p} and A_{mn}^{ku,t_q} can never be both equal to one, which, by Eq. (19), allows that W_{ku,t_q}^{ij,t_p} and W_{ij,t_p}^{ku,t_q} can be both equal to zero. Therefore, in this case of diverse routing, there is no spectrum overlapping constraint for these lightpaths.

E. MILP formulation without Traffic Grooming

The non-grooming formulation requires that any traffic in the network be routed by a single (direct) virtual link. Therefore, SSRs are required just in the source/destination nodes of each traffic and no longer at intermediate nodes as in the grooming approach. Since the added/dropped traffic are given as input to the MILP formulation and the number of SSRs used by a traffic on its source-destination nodes is the same independently of using grooming or not, the required number of SSRs is indifferent to the RMSA solution whenever grooming is not used.

The MILP formulation without grooming may be simplified through two major changes: *(i)* Eliminate the virtual topology constraints (grooming and regeneration constraints, (2)-(8); and *(ii)* Change all indices from (i-j) to (s-d), since the virtual links are obtained directly from the traffic matrix. With such simplification, $v^{s,d,t}$ is directly acquired from the traffic matrix parameters. The objective function remains the same, but without the second term.

4. HEURISTIC ALGORITHMS

Due to the complexity of the problem for large networks, the complete strategy presented in the proposed MILP formulation may be very time consuming. For instance, running the MILP formulation for the network shown in Fig. 1 (6-node topology) in an Intel i7 3.6GHz with 32GB of RAM machine took about 16 h for $T = 1$. For two additional VONs, the required simulation time increases considerably, which emphasizes that a heuristic model is necessary for moderate or large networks. The complexity of the complete MILP formulation may be reduced by decomposing the problem into two sub-problems: 1) the Virtual Topology desing (VTD) subproblem and 2) the RMSA subproblem. The first subproblem is proposed as a MILP formulation, whereas the second is based on heuristic algorithm. Each of them treats just part of the problem.

In the first subproblem (VTD), it is assumed that the VONs are known already. The source-destination pairs between which a certain number of virtual links ($b_{ij,t}$'s) are required to be established are taken as inputs. The virtual topologies can be created from a heuristic algorithm [1], as described in Subsection 4A, which determines the virtual links to be established and sets their corresponting $b_{ij,t}$ to 1 and they are an input parameter for the MILP formulation.

The second subproblem (RMSA) receives the set of virtual links ($b_{ij,t}$) as input and works to find the most appropriate route, a spectrally efficient modulation format and the set of contiguous and continuous slots in the physical substrate that best comply with the objective function directives. The RMSA solution can be determined by a heuristic algorithm, as described in Subsection 4A, which returns, for each virtual link, its routing ($A_{mn}^{ij,t}$), the initial slot ($s^{ij,t}$), the required modulation format ($\epsilon_z^{ij,t}$) and number of slots ($p^{ij,t}$).

Note that, by solving the subproblems in sequence and combining their solutions, we may end up not finding a solution as good as the one provided by the fully integrated problem, but the processing time may be substantially reduced while still acquiring a good solution. Obviously, a good solution will depend on the use of efficient strategies for each of the subproblems. The two subproblems together with their solution strategies are described in the next subsections.

A. Subproblem 1: Virtual Topology Design Heuristic (VTD - H)

This subproblem determines possible VONs for a given physical substrate. In other words, it selects a few source-destination node pairs between which virtual links need to be established. However, this subproblem is still concerned with the traffic routing between source-destination pairs over the virtual links, as the traffic routing is an integral part of the MILP (EQ9). Then, given the traffic matrix demands $\Lambda^{sd,t}$ and the virtual links $b_{ij,z}$, find for each virtual link their corresponding bandwidth $v^{ij,t}$ with a main objective function of minimizing the maximum virtual link' load, λ_{max}, along all virtual links over any VON with subformulation:

$$\min \qquad (\lambda_{max} + \theta . \sum_k SSR_k) \tag{26}$$

– ***subject to:***

$$v^{ij,t} \leq \lambda_{max} \qquad \forall (i,j), t \tag{27}$$

and constraints from Eq. (2) to Eq. (8) and from Eq. (22) to Eq. (25).

The offered traffic on a virtual link is defined as the sum of the traffic flow between those source-destination pairs that use this virtual link. The congestion over a VON should be kept to a minimum so that, as traffic scales up, minimimizing congestion will support future traffic growth. Therefore, Eq. (26) is a good objective function for the subformulation. The $v^{ij,t}$ found from the solution of subformulation will serve as input for the Subproblem 2, the RMSA.

B. Subproblem 2: Routing, Modulation Level and Spectrum Assignment (RMSA) Heuristic

Here, three alternative algorithms for solving the RMSA problem are presented; the first and the second are inspired by [24], whereas the third is an original metaheuristic proposal based on a Genetic Algorithm. The three approaches are described below.

B.1. Shortest Path With Maximum Spectrum Reuse With Modulation Constraints

Let us assume that a given set of path requests on t is given with their amount of requested traffic $v^{ij,t}$. The RMSA problem

can be solved by first turning this demand into the number of slots according to the distance (EQ10) between i and j and the modulation format spectral efficiency. Intuitively, the higher the slot reuse, the higher the reduction of the maximum number of required slots. In this section, it is proposed to use the shortest path with maximum spectrum reuse and modulation constraints (SP-M) algorithm, which combines the shortest path routing with the maximum reuse spectrum allocation (MRSA) algorithm shown in Algorithm 1 from [24]. In this approach, the spectrum path requests from every VON are first sorted according to the number of required slots, since the slot contiguity constraint makes it harder to find available consecutive slots for demands for a larger number of slots. After that, spectrum assignment is performed to the paths by following the order in which they were sorted. Note that only fiber-disjoint spectrum paths may reuse the same slots. We hence record the set of spectrum paths that are accommodated in the current iteration and employ a First-Fit strategy to find available consecutive slots spectrum assignment during the RMSA process.

B.2. Balanced Load Spectrum Allocation With Modulation Constraints:

In this subsection, we propose the use of another method, namely, balanced load spectrum allocation with modulation constraints (BL-M), which determines the routing by balancing the load within the network to potentially minimize the maximum number of used slots. As shown in the following three steps of the heuristic, BL-M also employs the First-Fit for spectrum assignment.

Step 1 Path generation: In this stage, we use the k shortest path algorithm to generate k ($k > 1$) paths, $P_h^{i,j}$, ($h = 1, 2, \ldots, k$), for each pair of nodes ij on VON t where there is a demanded spectrum path $v^{ij,t} > 0$.

Step 2 Path selection: In this stage, we decide the path for each demanded spectrum path, $v^{ij,t}$, with the goal of balancing the load among all fibers within the substrate network. The load of a fiber mn in the substrate network, L_{mn}, is estimated using Eq. (12) from [24]. The goodness of a path is evaluated by calculating the maximum fiber load ($C = \max_{mn} L_{mn}$) of the substrate network if the path is used to serve the demand for any VON. For a demanded spectrum path, all k candidate paths are tested. The candidate path that produces the lowest value of C is used as the routing path for the corresponding spectrum path. More specifically, starting from the spectrum path with the largest traffic demand, assign one of the k paths to it while minimizing C, until all the node pairs with non-zero traffic demands from all VONs are considered. After the path is selected, L_{mn} is updated according to Eq. (12) from [24]. For each analysed path, the modulation format (therefore the number of slots for the demand) with the highest spectral efficiency that meets the required distance of the path is selected.

Step 3: Spectrum allocation. In this stage, we use the First-Fit spectrum assignment strategy to accommodate all the spectrum paths for each VON and to find the number of required slots, C, of the network.

B.3. Our Proposed Genetic Algorithm (GA)

In this subsection, we describe in details our proposed genetic algorithm for the solution of the RMSA problem with multiple VONs. The algorithm is represented by the following steps:

1 **Initial Parameter Settings:** At this stage, some initial values are assigned to the input parameters. These parameters are:

1.1 **Population Size:** defines the number of individuals present at the admission of each GA generation.
1.2 **Number of generations:** defines how many iterations the GA will run;
1.3 **Elitism Index:** defines the number of best individuals stored and reinserted in population in each generation;
1.4 **Mutation Probability:** defines gene's chance of mutation at each individual;
1.5 **Physical Link Capacity (slots):** defines the number of available slots in each physical link;
1.6 **Bandguard Value:** Defined in Section 3B and represented by F.
1.7 **Set of k Alternate Paths:** Defines k paths provided for selection in the Routing step.
1.8 **Adjacency Matrix (graph):** defines the adjacency matrix of the physical network. The matrix size is $N \times N$, where N represents the network nodes and the value of each element is the distance (in km) among network nodes;
1.9 **Matrix of Demands:** defines the demands for each VON. Each element represents the demanded traffic flow (in Gb/s) from node i to node j in VON t, $v^{ij,t}$.
2 **Find k Shortest Paths for Each Demand:** using the parameters provided in the previous step (step 1), the algorithm performs the calculation of the k shortest-distance paths for each demand, using the well-known Yen's algorithm. The choice of this algorithm is due to the good performance and simplicity of its implementation. The algorithm returns two multi-dimensional arrays containing, respectively, the k paths and the k minimum distance (in km) for each demand. Thus, these two arrays have dimension $k \times ND$ (in which ND is the total number of demands for all VONs).
3 **Generate the initial population:** in this step, a set of P random individuals is generated, allowing a wide range of possible initial solutions. Each individual is represented by a line in the population matrix. This matrix is $P \times ND$, in which P is the population size and ND is the total number of demands. In addition, the value (among 1 and k) of each gene of the individuals represents one of the possible paths for that specific demand. Thus, each individual represents a possible solution to the problem. The following matrix (A_1) represents a possible routing solution for an hypothetical scenario with $k = 3$ and a certain amount of demands.

$$A_1 = \begin{bmatrix} 1 & 1 & 3 & 2 & 1 & 1 & 3 & 2 & \cdots & 2 \\ \vdots & \vdots & \vdots & \vdots & \vdots & \vdots & \vdots & \vdots & \ddots & \vdots \\ 3 & 1 & 1 & 2 & 3 & 2 & 1 & 1 & \cdots & 3 \end{bmatrix}, \quad \textbf{(28)}$$

4 **Calculate the individuals' fitness** in this step, the network is set up for each of the P input individuals and the fitness, defined as the maximum slot index, is found (EQ11) for each individual. To find this value, first the modulation format is calculated (EQ12) for each demand, then the demands are sorted according to the decreasing value of its spectrum necessity (considering the bandguard). After that, demands are allocated on the network using First-Fit spectrum allocation.
5 **Apply the Genetic Operators** in this step, the P individuals are ordered according to their evaluated fitness. All P individuals are passed to the crossover operation, which randomly combines them in pairs and applies a point-crossover operation through one, two or three intersection points in the set of genes of the individuals, with equal probability. Therefore, each new individual randomly inherits genes from a pair of parents and

P individuals generate $P/2$ new individuals. Fig. 4 depicts the crossover operation with two intersection points. The second genetic operator, the mutation function, uses the first half ($P/2$) of the population and alters one or more characteristics (genes) to one of the possible k path identifier, based on the mutation probability, provided as an input parameter. Therefore, $P/2$ individuals generate $P/2$ new individuals. It is worth mentioning that all probability parameters used in the simulation were set empirically. Fig. 5 depicts the mutation operator applied to a hypothetical individual.

6 **Apply Elitism** Before the crossover and mutation operators, a percentage of the fittest individuals in P are stored in a set I. During the crossover step, P individuals are combined in pairs to form $P/2$ new individuals, whereas in the mutation process $P/2$ mutated individuals form $P/2$ new individuals. These P new individuals are combined with the previously stored I best individuals of P and an elitism process is performed to generate P individuals, and a new generation (step 4) is originated.

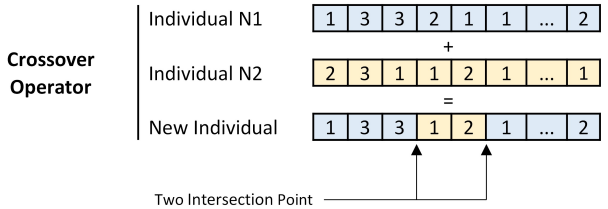

Fig. 4. Graphical example of the crossover genetic operator applied to a pair of hypothetical individuals. In the example it was considered two intersection points.

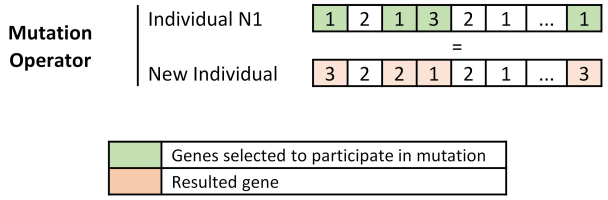

Fig. 5. Graphical example of the mutation genetic operator applied to an hypothetical individual.

The heuristic algorithm can be considered with or without grooming. Note that, for the non-grooming approach, only subproblem 2 must be solved, since the $v^{ij,t}$ are obtained from the original traffic matrices and are mapped directly onto the physical substrate.

5. SIMULATIONS AND RESULTS

In this section we show some results obtained by the use of the complete MILP formulations with and without grooming, as well as by the heuristic algorithms.

A. Small Network

To test the effectiveness of the MILP formulation and heuristics proposed in Section 3 and Section 4, respectively, a number of simulations from small, but representative, networks are tested. The slot width, $\Omega = 12.5\ GHz$, the filter guard band between wavebands is of one slot, θ=0.001 and $R = 100$ Gb/s for all simulations. Four modulation formats ($|M| = 4$) are considered. For each modulation z, data rate-to-bandwidth ratios, η_z, are: $\eta_1 = 1$, $\eta_2 = 2$, $\eta_3 = 3$ and $\eta_4 = 4$ bit/s/Hz and maximum reach of the lightpaths are $d_1 = 4000$ km, $d_2 = 2000$ km, $d_3 = 1000$ km and $d_4 = 500$ km, respectively. The GA meta-heuristic is tuned with mutation rate= 0.2, number of generations = 800 and number of individuals = 600. The simulations were performed using the MILP formulation or/and heuristic with and without grooming for 1 virtual topology (T=1) or 3 virtual topologies (T=3) over a single physical substrate (6 nodes network illustrated in Fig. 1). The MILP simulation used the IBM ILOG CPLEX solver [25] and ran on an Intel i7 3.6GHz with 32GB of RAM.

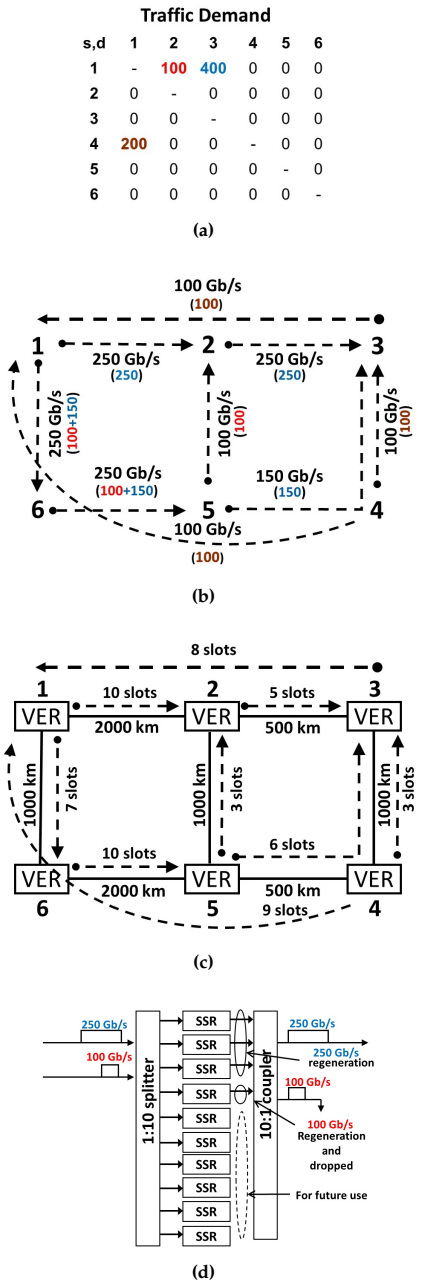

Fig. 6. (a) Demand (b) Grooming (c) RMSA (d) VER example at node 2

A.1. Case 1 (6-node network with T= 1 and 3 demands)

In order to facilitate the reader's understanding, firstly we consider the results of the simulation for a simple example. Consider a 6-node network (Fig. 6) with three traffic demands: 100 Gb/s between nodes 1 and 2 (red); 200 Gb/s between nodes 4 and 1

Table 2. Results for $T = 1$

MILP					
Node	Grooming				Non-Grooming
	ri_k	ro_k	SSR_k	C	C
1	8	8	8		
2	12	12	12		
3	7	7	7	16	31
4	5	5	5	(∼ 16h)	(503s)
5	10	10	10		
6	8	8	8		

Table 3. Results for $T = 1$

HEURISTICS							
Node	Grooming VTD-H				Non-Grooming		
	ri_k	ro_k	SSR_k	(GA-C)	(GA-C)	(BL-M C)	(SP-M C)
1	7	7	7				
2	12	12	12				
3	6	6	6	16	35	36	36
4	6	6	6	(gap=0%)	(gap=12%)	(gap=13.8%)	(gap=13.8%)
5	12	12	12	(<10s)	(<10s)	(<10s)	(<10s)
6	7	7	7				

Table 4. Results for $T = 3$

MILP					
Node	Grooming				Non-Grooming
	ri_k	ro_k	SSR_k	C	C
1	21	21	21		
2	31	31	31		
3	18	18	18	50*	97*
4	23	23	23		
5	33	33	33		
6	21	21	21		

Table 5. Results for $T = 3$

HEURISTICS							
Node	Grooming VTD-H				Non-Grooming		
	ri_k	ro_k	SSR_k	(GA-C)	(GA-C)	(BL-M C)	(SP-M C)
1	23	23	23				
2	39	39	39				
3	20	20	20	50	99	100	100
4	21	21	21	(gap*=0%)	(gap*=2.02%)	(gap*=3%)	(gap*=3%)
5	40	40	40	(<10s)	(<10s)	(<10s)	(<10s)
6	23	23	23				

(brown); and 400 Gb/s between nodes 1 and 3 (blue) and virtual topology (dashed lines in Fig. 6b) and physical topology (Fig. 6c) with VERs in its nodes. Note that the brown traffic, added at node 4 and dropped at node 1, could be sent directly because there is a virtual link between these node. However, as the MILP has the objective to minimize the spectrum use, it returns a solution where the brown traffic is partitioned: half of the traffic (100 Gb/s) is sent directly by virtual link 4-1 and the other half is sent by virtual links 4-3 and 3-1. Therefore, the half of traffic carried on the two individual virtual links undergoes electronic processing between the two virtual links at node 3. Similar MILP arrangements can be seen for the blue and red traffic demands. The VER configuration at node 2 is presented in Fig. 6d. For this example, we could set up node 2 with 4 SSRs ($SSR_2 = 4 = max(ri_2 = 3, ro_2 = 4)$), despite the figure shows the availability of 10 SSRs.

Note the maximal link load over any physical link is 250 Gb/s. This differs from a possible design without grooming, where there is no electronic processing at intermediate nodes and no traffic partitioning. In the later case, the maximal link load over any physical link would be at least 400 Gb/s.

A.2. Case 2 (6-node network with T=1 and several demands)

For this analysed scenario, we have simulated two cases: one with grooming and the other without grooming. For each of them, there is a single virtual topology (T=1). The virtual topology over the physical substrate is simulated with a traffic matrix, such that each node demands 100 Gb/s for every other node, that is $\Lambda^{sd,1} = 100$ Gb/s $\forall s, d$.

Tables 2 and 3 show the values of SSR_k found for each node k and the resulting performance in terms of the maximum number of frequency slots, C, among all fiber links in the substrate network for the complete MILP formulation, as well as for the heuristic solutions. As can be seen, in all reported cases, grooming requires considerably less spectrum resources than the non-grooming scenario and the GA heuristic has slightly better performance than the other techniques. In addition, it can be seen that, with grooming, the maximum number of frequency slots in the network links (C) has been reached by the MILP and heuristic solutions. Also the heuristic with grooming reached the same number of total SSRs ($\sum_k SSR_k = 50$) as the MILP. With respect to optimality gap, we noted that it is 0 for GA with grooming and less than 14% for the approaches without grooming. T=1 with grooming, as expected, is the case with lowest spectrum requirement, but is subject to not providing any additional virtual topology.

A.3. Case 3 (6-node network with T=3 and several demands)

The complexity for the solution grows quickly as the number of variables increases. However, by deploying multiple VONs, an operator will have the capability to partition its physical substrate into several independent VONs. That is very important, because each VON can have different bandwidth, QoS capability etc. The partitioning criteria can be defined based on user or application requirements.

Again we simulate both the grooming and non-grooming cases. For each of them, there are three virtual topologies (T=3) over the same physical substrate. The simulation uses three

traffic matrices, $\Lambda^{sd,t}$ with t=1,2,3, but, for each, a node demands 100 Gb/s to be sent to every other node, that is $\Lambda^{sd,t} = 100$ Gb/s $\forall sd, t$. Comparing the results for the grooming and non grooming scenarios in Tables 4 and 5, we observe a clear gain in terms of saved bandwidth for the grooming approach. The MILP formulation with grooming reached that with a lower number of SSRs than the heuristic (147 against 166), which results in a reduction of around 11.4%.

Because of the complexity of the problem with T=3, the complete MILP is very time consuming. For instance, running the MILP formulation (without grooming) for the 6-node network for 8h, the CPLEX solver does not find any solution; running for 24h the solution is C=97. Finally, if we run for 3 days, the solution still is C=97 and that was our limit time (stopping criterion) for the CPLEX solver. Therefore, in Table 5, we can seen that the gap* with that limit time is 0 for grooming whereas it is around 2% with GA non-grooming and 3% with BL-M and SP-M heuristics without grooming. Again, the GA heuristic performs slightly better than the other techniques.

A.4. Case 4 (6-node network with T=1 and several different demands)

We simulate grooming and non-grooming cases with MILP for (T=1) with uniform distribution between 20 and 100 Gb/s. It means that each node demands 20, 40, 60 or 100 Gb/s to be sent to every other node and in this case the traffic matrix will referred to as "rand". The number of SSRs is showed in Table 6. Again, we observe a clear gain in terms of saved bandwidth for the grooming approach, 11 against 23. The Fig. 7 also compares the "rand" demand to the source-destination pair with fixed demands (20, 40, 60, 80 or 100 Gb/s). The amount of spectrum is as expected: an intermediate value between the findings for the fixed demands.

A.5. Case 5 (6-node network with several VONs with different demands)

To assess the performance of the GA with several VONs (5, 10, 15 and 20), we simulate the grooming approach with uniform distribution between 20 and 100 Gb/s for the demands. The results, as shown in Fig. 8, indicate the increase of used spectrum and total number of SSRs in function of number of VONs. The CPU time was 9 min for 5 VONs and increased significantly to 40 min with 20 VONs.

Table 6. Results for $T = 1$ with random (s,d) pair demand (20, 40, 60, 80 or 100 Gb/s)

MILP					
Node	Grooming				Non-Grooming
	ri_k	ro_k	SSR_k	C	C
1	5	5	5		
2	7	7	7		
3	5	4	5	11	23
4	6	6	6		(67s)
5	8	8	8		
6	4	5	5		

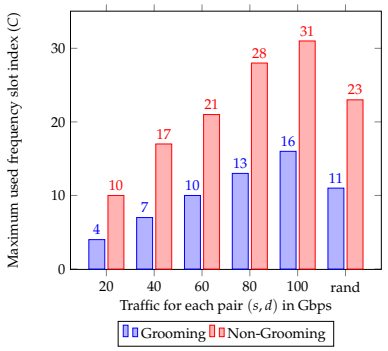

Fig. 7. Spectrum used in function of traffic

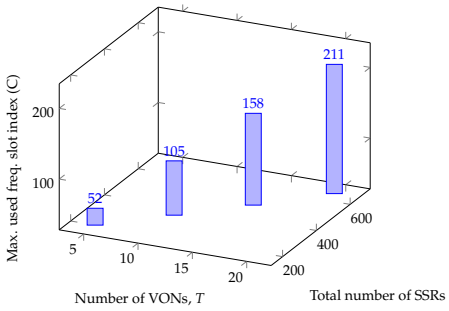

Fig. 8. Total number of SSRs and spectrum used in function of several VONs with different rand traffic and grooming (approach: VTD-H with GA)

B. Large Networks

When a large number of variables are involved, the processing time of the MILP formulation is not viable, so, for large networks, only the heuristics are investigated. Several networks are studied (12 in total) where the physical distance between the nodes and the physical substrate are presented in Fig. 9. Again the traffic matrices for each virtual topology were generated with $\Lambda^{sd,t}$ equal to 100 Gb/s for all pair s-d over all VONs.

The slot width, Ω, and the filter guard band between wavebands of one slot is 12.5 GHz. Four modulation formats ($|M| = 4$) are considered. For each modulation z, data rate-to-bandwidth ratios, η_z, are: $\eta_1 = 1$, $\eta_2 = 2$, $\eta_3 = 3$ and $\eta_4 = 4$ bit/s/Hz and the maximum reach of the lightpaths are $d_1 = 8000km$, $d_2 = 2000km$, $d_3 = 1000km$ and $d_4 = 500km$ respectively. Pre-determined VONs are assumed for the grooming with the VTD-H heuristic, with an average virtual degree similar to the nodal degree of the network using a similar strategy to the first phase of the minimum-delay logical topology design algorithm (MLDA) heuristic from [1]. This strategy is capable of satisfying the tightest delay constraints that are physically realizable. That is important for virtual topologies due to practical latency constraints.

Table 7 compares the maximum slot index (C) returned by the optical grooming approach and the non-grooming scheme for the 12 analysed topologies. For the grooming approach, we decided to use only the GA in the RMSA subproblem, because our final objective is to minimize the load (the maximum offered load to a virtual link) and the GA has shown better performance than the other algorithms. For all cases the GA meta-heuristic is tuned with mutation rate= 0.2, number of generations = 800 and number of individuals = 600. The grooming approach achieves significantly better performance in all of the networks compared

Table 7. REAL-WORLD REFERENCE NETWORKS http://www.av.it.pt/anp/on/refnet2.html - utilized spectrum slot index "C" in the network and each model/heuristic considering $|M| = 4$ modulation format, $T = 1$ and $T = 3$ virtual topologies. Number of nodes and links are indicated by N and L.

Network id	Name	N (number of nodes)	L (links)	Nodal Degree (mean)	Grooming		Non Grooming					
					VTD-H(GA)		(GA)		(BL-M)		(SP-M)	
					T=1	T=3	T=1	T=3	T=1	T=3	T=1	T=3
					C	C	C	C	C	C	C	C
1	8-NODES NET	8	2x12	3	11	35	25	67	27	70	35	98
2	METRO	10	2x16	3.2	21	65	32	95	35	98	38	107
3	ABILENE	11	2x14	2.55	60	182	130	362	145	386	187	553
4	PAN EUROP	11	2x26	4.72	10	32	22	71	27	71	62	158
5	FINLAND	12	2x19	3.16	24	74	55	160	57	163	86	248
6	BRAZILIAN	12	2x20	3.33	35	107	76	220	86	249	112	281
7	NSFNET	14	2x21	3	98	296	115	342	144	371	189	554
8	JAPAN	14	2x22	3.15	33	101	71	201	71	201	82	235
9	DEUTSCHE	14	2x23	3.28	27	83	57	177	69	200	75	217
10	PACIFIC BELL	17	2x23	2.7	100	314	196	553	196	553	221	584
11	EON	19	2x38	4	136	410	176	530	221	589	266	744
12	USA	24	2x43	3.58	256	610	328	963	355	981	585	1721

to the non-grooming scheme as shown by the total maximum spectrum index of the grooming and non-grooming schemes. Also, when we compare the results of the RMSA when grooming is not used, it can be seen that the GA used fewer slots than BL-M and SP-M for most of the analysed topologies and either $T = 1$ or $T = 3$, except for Japan, Pacific Bell and PAN EUROP networks (with $T = 3$). For instance, for most of the cases, reductions of about 20% were achieved with the use of the GA instead of BL-M (for example, NSFNET) with $T = 1$. In all analyzed cases, we can confirm that SP-M does not balance the load as efficiently as BL-M, which needs additional overhead and thus requires more slots for every case. Therefore, the comparison between GA, BL-M and SP-M indicates that GA and BL-M can indeed achieve superior load balancing in the network and therefore superior results when the network maximum slot index reduction is the aim.

Table 8 also shows the results for a single virtual toplogy case (T=1) in terms of the number of SSRs requested for each node with VER. For example, for the eight node network Node 1 required 7 SSRs and Node 8 required 12 SSRs whereas for the USA network Node 1 required 23 SSRs and Node 19 required 50 SSRs.

B.1. Further results with modified objectives

By using the objective function (26) in VTD-H, the optimization process tends to minimize the utilised spectrum over any link, and most of works in literature consider that objective. However, in reality, it is also important to decrease the design cost because in many cases budget is limited, especially in terms of final equipment, including the SSRs. For example, for the PAN-E network, we can see in Table 8 a high number of requested SSRs (204 in total).

To solve this problem, we can change the objective such that the main objective function is the total number of SSRs, referred to as OBJ 2.

$$\min \quad (\sum_k SSR_k + \theta.\lambda_{max}) \tag{29}$$

and maintaining the constraints (2) to (8).

Additionally, the designer could be interested in limiting the maximum number of SSRs in a node. For example, for the USA network, Node 9 required 143 SSRs. To solve this problem, the objective function can be changed. We then create a variable, $MaxSSR$, to designate the maximum number of SSRs per node. The grooming subproblem in the heuristic form is then solved with a new objective function that emphasizes the reduction of the maximum number of interfaces in each network node, referred to as OBJ 3:

$$\min \quad (MaxSSR + \theta.\lambda_{max}) \tag{30}$$

– ***subject to:***

$$SSR_k \leq MaxSSR \qquad \forall k \in N \tag{31}$$

and maintaining the constraints (2) to (8).

In order to assess the two new objective functions, simulations were performed with each of them. Tables 9 and 10 show an overview of the number of SSRs for the 12 networks for OBJ 2 and OBJ 3, respectively. The total number of SSRs, $\sum_k SSR_k$, is denoted as n_t. Note that, under the same traffic matrix as in the previous analysis, the total number of requested SSRs in the PAN-E network decreased to 172 with the OBJ 2 compared to OBJ 1 ($n_t = 204$); and, for the USA network with OBJ 3, Node 9 requested only 95 SSRs against 143 with OBJ 1.

We can observe that the OBJ 2 approach always has the better performance in terms of the total number of SSRs in relation to OBJ 1 or OBJ 3, since the OBJ 2 approach employs one

fundamental change in objective function: aiming to minimize n_t, the total number of SSRs. It can be observed that ABIL, JAPAN, PA.BE and EON networks have identical results; EIGHT, METRO, FINLA and USA obtain an increase in the number of SRRs blocks of less than 3%; BRAZ, NSF, and DT of less than 8% and just FINLA, with 18.6%, presented a high increase. It is apparent from the analysis of the Tables 8 and 9 that in general there are very few changes in n_t when changing from OBJ 1 and OBJ 2 across several networks, as can be seen from the box plots in Fig. 10. The results suggest that OBJ 1 is a good objective function, since it acquires the lowest possible number of required slots in the network links and also results in a number of SSRs close to the minimum possible value.

OBJ 3 limits the maximum number of SSRs in each node. For example, it can be observed in Tables 8 and 10 that OBJ 3 over the USA network requires at most 95 SSRs in any single node, whereas using OBJ 1 up to 143 SSRs are required in a node. Note as well that, according to Table 9, if a metric that aims to reduce the total number of SSR blocks, as in OBJ 2, is used in the USA network, up to 142 SSRs blocks are required in a node. Despite the maximimum limit on the number of SSR blocks in a node imposed by OBJ 3, it has the effect of increasing the number of SSRs over some nodes in relation to OBJ 1 and that could be critical. For example, in the same USA network, there is an increase in number of requested SSRs per node in 13 out of 24 nodes. While this is true for several cases, interestingly, it is not for all; for example, in the PAN-E network, despite the maximum number of SSRs is determined to be 16 with OBJ 3, the total number of SSRs also decreases in relation to the result of OBJ 1. Taken together, these results suggest that the impact of the modified objectives could have an association between the network connectivity and the objective functions.

6. CONCLUSION

The main goal of the current study was to determine the planning of elastic optical networks with virtualization and grooming, considering virtual elastic lightpaths and virtual regenerators. A MILP formulation is developed to solve the virtual topology design (EQ22) and RMSA problems jointly with grooming, different modulation formats and no pre-calculated routes. Heuristic algorithms are proposed to provide solutions for large networks. Results show that the MILP formulation with grooming and the proposed heuristic strategies are efficient for saving resources such as spectrum and virtual elastic regenerators. For example, the VTD-H heuristic with GA for the small network studied with a VON has optimality gap equal to zero, however with less computational time (EQ23). For three VONs the optimality gap is expected to be low as well. Therefore, this kind of planning (combining grooming and routing) can achieve a better performance than the traditional EON virtualization problem. These findings confirm the association between virtualization and grooming in EONs (grooming saving range from about 20% to about 50% in relation to non-grooming in cases studied for large networks). A natural progression of this work is to examine more closely the links between the different objective functions, maybe with multiobjective techniques solved through new heuristics. It would also be interesting to assess the effects of energy efficiency over the final topology as well as survivability due to failure using the approaches studied in this paper (EQ24).

ACKNOWLEDGMENTS

This study was financed in part by the Coordenação de Aperfeiçoamento de Pessoal de Nível Superior - Brasil (CAPES) - Finance Code 001. Thanks are also directed to CNPq-Brasil, FAPESB-Brasil and FACEPE-Brasil, Federal University of Bahia, Federal University of Recôncavo da Bahia, Federal University of Pernambuco, Concordia University, High Performance Networks group and Smart Internet Lab of Bristol University. The writers are indebted to their colleague (EQ20) at the Laboratory, Mr. Leonardo Dias, for many helpful suggestions during the course of the GA algorithm implementation.

REFERENCES

1. R. Ramaswami and K. N. Sivarajan, "Design of logical topologies for wavelength-routed optical networks," IEEE J. on Sel. Areas Commun. **14**, 840–851 (1996).
2. T. E. Stern and K. Bala, *Multiwavelength optical networks: a layered approach* (Addison-Wesley Longman Publishing Co., Inc., 1999).
3. A. Hammad, R. Nejabati, and D. Simeonidou, "Novel approaches for composition of online virtual optical networks utilizing o-ofdm technology," in *39th European Conference and Exhibition on Optical Communication (ECOC 2013)*, (2013), pp. 1–3.
4. L. Gong and Z. Zhu, "Virtual optical network embedding (vone) over elastic optical networks," J. Light. Technol. **32**, 450–460 (2014).
5. N. Shahriar, S. Taeb, S. R. Chowdhury, M. Tornatore, R. Boutaba, J. Mitra, and M. Hemmati, "Achieving a fully-flexible virtual network embedding in elastic optical networks," in *IEEE INFOCOM 2019 - IEEE Conference on Computer Communications*, (2019), pp. 1756–1764.
6. H. Duong and B. Jaumard, "A nested decomposition model for reliable nfv 5g network slicing," in *9th International Network Optimization Conference Avignon, France, June 12–14, 2019*, (2019), p. 107.
7. M. Jinno, H. Takara, K. Yonenaga, and A. Hirano, "Virtualization in optical networks from network level to hardware level," J. Opt. Commun. Netw. **5**, A46–A56 (2013).
8. K. Christodoulopoulos, I. Tomkos, and E. A. Varvarigos, "Elastic bandwidth allocation in flexible ofdm-based optical networks," J. Light. Technol. **29**, 1354–1366 (2011).
9. V. Abedifar, M. Furdek, A. Muhammad, M. Eshghi, and L. Wosinska, "Routing, modulation, and spectrum assignment in programmable networks based on optical white boxes," IEEE/OSA J. Opt. Commun. Netw. **10**, 723–735 (2018).
10. K. Assis, R. Almeida, H. Waldman, A. Santos, M. Alencar, M. Reed, A. Hammad, and D. Simeonidou, "Sla formulation for squeezed protection in elastic optical networks considering the modulation format," IEEE/OSA J. Opt. Commun. Netw. **11**, 202–212 (2019).
11. M. Jinno, K. Yonenaga, H. Takara, K. Shibahara, S. Yamanaka, T. Ono, T. Kawai, M. Tomizawa, and Y. Miyamoto, "Demonstration of translucent elastic optical network based on virtualized elastic regenerator," in *National Fiber Optic Engineers Conference*, (Optical Society of America, 2012), pp. PDP5B–6.
12. Y. Zhao, B. Chen, J. Zhang, and X. Wang, "Energy efficiency with sliceable multi-flow transponders and elastic regenerators in survivable virtual optical networks," IEEE Transactions on Commun. **64**, 2539–2550 (2016).
13. A. N. Patel, C. Gao, J. P. Jue, X. Wang, Q. Zhang, P. Palacharla, and T. Naito, "Cost efficient traffic grooming and regenerator placement in impairment-aware optical wdm networks," Opt. Switch. Netw. **9**, 225–239 (2012).
14. Z. Cai, F. Liu, N. Xiao, Q. Liu, and Z. Wang, "Virtual network embedding for evolving networks," in *2010 IEEE Global Telecommunications Conference GLOBECOM 2010*, (2010), pp. 1–5.
15. K. D. R. Assis, L. A. J. Mesquita, R. C. Almeida, H. Waldman, A. Hammad, and D. Simeonidou, "Virtualisation of optical networks utilising squeezing protection: the exact formulation," Electron. Lett. **55**, 1098–1101 (2019).
16. N. Shahriar, S. Taeb, S. R. Chowdhury, M. Zulfiqar, M. Tornatore,

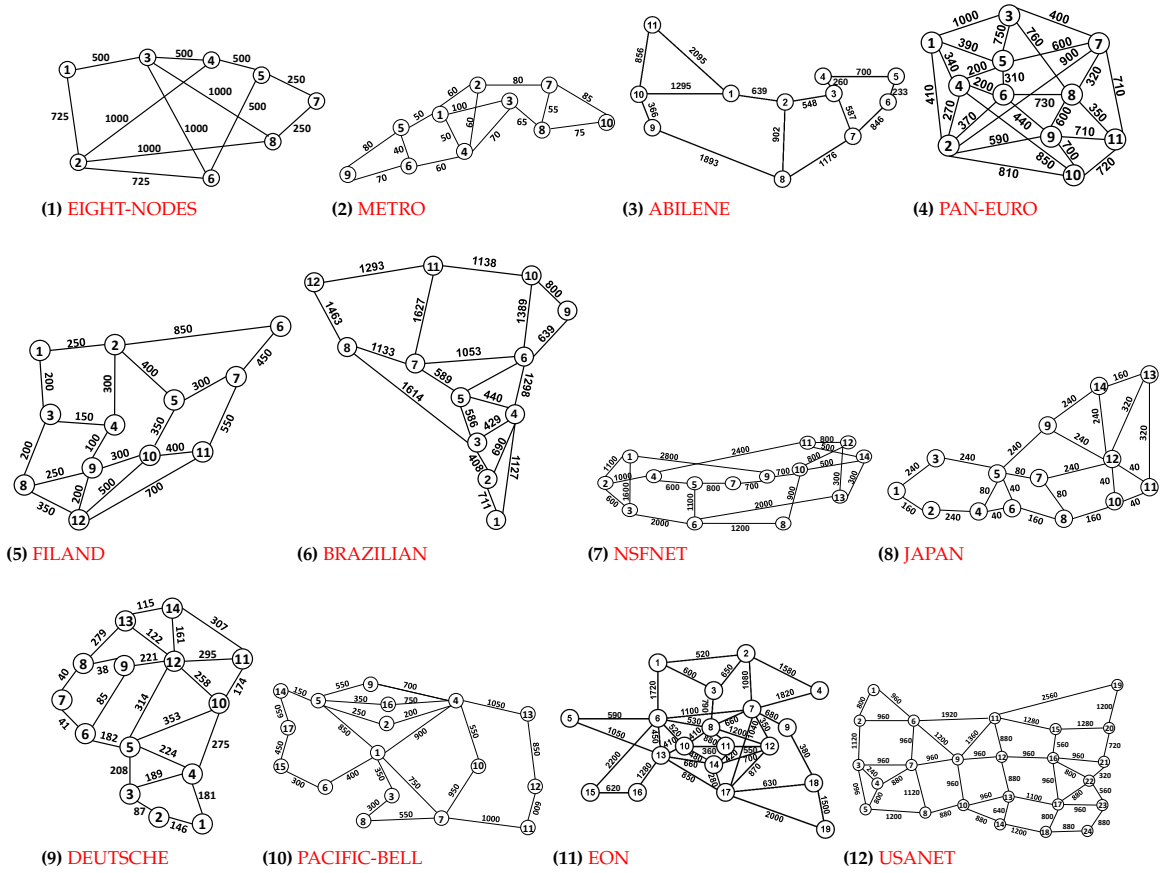

Fig. 9. 12 physical topologies over study

R. Boutaba, J. Mitra, and M. Hemmati, "Reliable slicing of 5g transport networks with dedicated protection," arXiv preprint arXiv:1906.10265 (2019).

17. K. D. R. Assis, S. Peng, R. C. Almeida, H. Waldman, A. Hammad, A. F. Santos, and D. Simeonidou, "Network virtualization over elastic optical networks with different protection schemes," IEEE/OSA J. Opt. Commun. Netw. **8**, 272–281 (2016).
18. G. Zhang, M. De Leenheer, and B. Mukherjee, "Optical traffic grooming in ofdm-based elastic optical networks [invited]," IEEE/OSA J. Opt. Commun. Netw. **4**, B17–B25 (2012).
19. M. Jinno, Y. Sone, H. Takara, A. Hirano, K. Yonenaga, and S. Kawai, "Ip traffic offloading to elastic optical layer using multi-flow optical transponder," in *2011 37th European Conference and Exhibition on Optical Communication,* (2011), pp. 1–3.
20. H. Wang and G. N. Rouskas, "Traffic grooming in optical networks: Decomposition and partial linear programming (lp) relaxation," IEEE/OSA J. Opt. Commun. Netw. **5**, 825–535 (2013).
21. H. Wang and G. N. Rouskas, "Hierarchical traffic grooming: A tutorial," Comput. Networks **69**, 147 – 156 (2014).
22. P. Soto, P. Maya, and J. F. Botero, "Resource allocation over eon-based infrastructures in a network virtualization environment," IEEE Transactions on Netw. Serv. Manag. **16**, 13–26 (2019).
23. M. Jinno, T. Takagi, and K. Kiyokawa, "Minimal virtualized-elastic-regenerator placement and least congestion resources assignment for translucent elastic optical networks," in *Optical Fiber Communication Conference,* (Optical Society of America, 2015), pp. Th3J–2.
24. Y. Wang, X. Cao, and Y. Pan, "A study of the routing and spectrum allocation in spectrum-sliced elastic optical path networks," in *2011 Proceedings Ieee Infocom,* (IEEE, 2011), pp. 1503–1511.
25. ILOG, IBM, "CPLEX optimizer," [online]. Available: http://www-01.ibm.com/software/commerce/optimization/cplex-optimizer (2012).

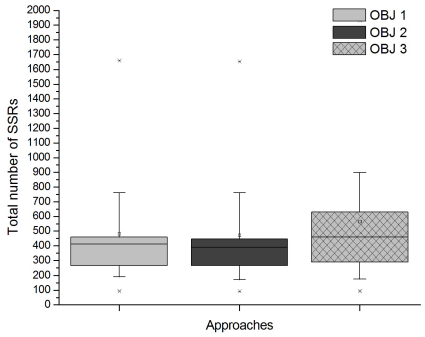

Fig. 10. Box plot of the number of SSRs blocks in each objective function

Table 8. OBJ 1. Utilized subregenerators "SRR_k" for each node k for each network considering $T = 1$

	Node k	1	2	3	4	5	6	7	8	9	10	11	12	13	14	15	16	17	18	19	20	21	22	23	24	n_t
1	EIGHT	7	16	15	12	12	12	8	12	.	.	.	.	.	.	.	.	.	.	.	.	.	.	.	.	94
2	METRO	25	26	26	26	17	18	17	17	9	9	.	.	.	.	.	.	.	.	.	.	.	.	.	.	190
3	ABIL	25	36	35	18	12	18	35	35	23	19	10	.	.	.	.	.	.	.	.	.	.	.	.	.	266
4	PAN E	15	24	16	20	19	20	20	20	19	15	16	.	.	.	.	.	.	.	.	.	.	.	.	.	204
5	FINLA	18	36	24	24	23	18	23	22	25	26	23	22	.	.	.	.	.	.	.	.	.	.	.	.	284
6	BRAZ	11	16	29	33	34	41	33	26	11	19	22	14	.	.	.	.	.	.	.	.	.	.	.	.	289
7	NSF	22	25	27	38	37	51	19	24	31	43	27	23	23	21	.	.	.	.	.	.	.	.	.	.	411
8	JAPAN	16	25	25	42	71	35	36	36	33	30	14	53	14	16	.	.	.	.	.	.	.	.	.	.	446
9	DT	16	15	33	48	62	33	16	7	25	28	43	19	63	33	19	.	.	.	.	.	.	.	.	.	460
10	PA.BE	112	35	28	100	74	42	66	18	17	28	32	25	35	42	25	16	25	.	.	.	.	.	.	.	720
11	EON	33	36	24	18	18	83	99	57	26	36	23	34	64	33	25	25	82	26	18	.	.	.	.	.	760
12	USA	23	35	47	24	23	126	123	69	143	125	120	95	95	66	56	104	97	53	50	36	40	46	39	23	1658

Table 9. OBJ 2. Utilized subregenerators "SRR_k" for each node k for each network considering $T = 1$

	Node k	1	2	3	4	5	6	7	8	9	10	11	12	13	14	15	16	17	18	19	20	21	22	23	24	n_t
1	EIGHT	8	16	13	9	12	12	9	13	.	.	.	.	.	.	.	.	.	.	.	.	.	.	.	.	92
2	METRO	26	25	26	24	18	16	16	17	9	9	.	.	.	.	.	.	.	.	.	.	.	.	.	.	186
3	ABIL	26	35	37	20	12	16	35	33	22	20	10	.	.	.	.	.	.	.	.	.	.	.	.	.	266
4	PAN E	12	20	14	15	15	20	20	17	15	12	12	.	.	.	.	.	.	.	.	.	.	.	.	.	172
5	FINLA	17	34	24	24	22	17	23	21	22	25	23	24	.	.	.	.	.	.	.	.	.	.	.	.	276
6	BRAZ	11	16	31	30	30	37	29	22	11	17	23	15	.	.	.	.	.	.	.	.	.	.	.	.	272
7	NSF	23	23	25	33	31	49	19	19	33	39	27	29	25	15	.	.	.	.	.	.	.	.	.	.	390
8	JAPAN	15	21	27	39	72	33	37	34	36	26	15	53	14	18	.	.	.	.	.	.	.	.	.	.	446
9	DT	16	15	32	41	57	29	14	24	31	39	15	70	28	15	.	.	.	.	.	.	.	.	.	.	426
10	PA.BE	107	29	29	108	69	42	65	20	16	37	27	19	34	42	28	20	28	.	.	.	.	.	.	.	720
11	EON	28	36	23	18	18	91	93	56	22	39	21	41	64	34	24	24	84	26	18	.	.	.	.	.	760
12	USA	23	33	45	27	32	122	116	70	142	126	106	98	93	68	44	110	94	59	47	42	48	47	37	23	1652

Table 10. OBJ 3. Utilized subregenerators "SRR_k" for each node k for each network considering $T = 1$

	Node k	1	2	3	4	5	6	7	8	9	10	11	12	13	14	15	16	17	18	19	20	21	22	23	24	n_t
1	EIGHT	7	14	14	11	14	11	10	13	.	.	.	.	.	.	.	.	.	.	.	.	.	.	.	.	94
2	METRO	24	24	24	24	24	24	24	24	15	15	.	.	.	.	.	.	.	.	.	.	.	.	.	.	222
3	ABIL	30	30	30	27	30	27	30	30	29	30	18	.	.	.	.	.	.	.	.	.	.	.	.	.	311
4	PAN E	16	16	16	16	16	16	16	16	16	16	16	.	.	.	.	.	.	.	.	.	.	.	.	.	176
5	FINLA	14	27	27	26	25	15	27	23	27	27	23	27	.	.	.	.	.	.	.	.	.	.	.	.	288
6	BRAZ	13	25	29	28	28	28	29	28	21	24	29	20	.	.	.	.	.	.	.	.	.	.	.	.	302
7	NSF	37	26	37	37	34	37	26	15	37	37	37	35	37	27	.	.	.	.	.	.	.	.	.	.	459
8	JAPAN	36	44	26	48	48	46	48	48	45	48	48	48	48	48	.	.	.	.	.	.	.	.	.	.	629
9	DT	45	45	45	45	45	45	37	45	40	45	45	41	45	39	.	.	.	.	.	.	.	.	.	.	607
10	PA.BE	74	33	42	75	75	52	74	40	20	32	48	51	45	52	52	25	52	.	.	.	.	.	.	.	842
11	EON	42	56	56	18	20	62	62	62	42	48	38	62	62	53	43	43	62	43	25	.	.	.	.	.	899
12	USA	25	77	93	48	77	95	90	95	95	95	95	95	95	84	79	95	95	78	44	83	81	88	71	59	1932